JCAMECH

Vol. 50, No. 1, June 2019, pp 182-190
DOI: 10.22059/jcamech.2019.276606.365

Dynamical stability of cantilevered pipe conveying fluid in the presence of linear dynamic vibration absorber

Z.Y. Liu[a,b], K. Zhou[a,b], L. Wang[a,b,] ∗ *,T.L. Jiang[a,b] and H.L.Dai[a,b]*

[a] *Department of Mechanics, Huazhong University of Science and Technology, Wuhan 430074, China*
[b] *Hubei Key Laboratory for Engineering Structural Analysis and Safety Assessment, Wuhan 430074, China*

ARTICLE INFO

Article history:
Received: 23 February 2019
Accepted: 26 March 2019

Keywords:
Pipe conveying fluid
Linear dynamic vibration absorber
Stability
Critical flow velocity
Nonlinear oscillation

ABSTRACT

When the velocity of fluid flow in a cantilevered pipe is successively increased, the system may become unstable and flutter instability would occur at a critical flow velocity. This paper is concerned with exploring the dynamical stability of a cantilevered fluid-conveying pipe with an additional linear dynamic vibration absorber (DVA) attachment. It is endeavoured to show that the stability of the pipe may be considerably enhanced due to the presence of DVA. The quasi-analytical results show that the energy transferred from the flowing fluid to the pipe may be partially transferred to the additional mass. In most cases, thus, the critical flow velocity at which the pipe becomes unstable would become larger, meanwhile the flutter instability of the DVA is not easy to achieve. In such a fluid-structure interaction system, it is also found that flutter instability may first occur in the mode of the DVA. The effects of damping coefficient, weight, location and spring stiffness of the DVA on the critical flow velocities and nonlinear oscillations of the system have also been analyzed.

1. Introduction

Since the 1950s, the dynamics of pipes conveying fluid has become a hot topic in the research fields of fluid-structure interactions as well as dynamical systems. In an excellent review provided by Paidoussis and Li[1], it was shown that the pipe conveying fluid has become a model dynamical problem. Indeed, the system of fluid-conveying pipe has established itself as a generic paradigm of a kaleidoscope of interesting dynamical behavior[1]. In 2008, Paidoussis[2] further discussed the radiation of the experience gained in studying the problem of pipes conveying fluid into other areas of Applied Mechanics, particularly other problems in fluid-structure interactions. Interestingly, the dynamical system of pipes at microscale or nanoscale has also been analyzed by many researchers (see, e.g., [3, 4]). Thus, the literature on this topic is very extensive and is still constantly expanding. The dynamical behaviors of pipes with supported ends, clamped-free ends or with unusual boundary conditions; articulated rigid pipes or continuously flexible pipes; pipes conveying incompressible or compressible fluid, with steady or unsteady flow velocity; linear, nonlinear and chaotic dynamics; these and many more have been the object of research in the past decades[1].

The question of the existence of buckling (divergence) instability of fluid-conveying pipes supported at both ends has been answered in several early papers [5-7], where the linear equations of motion were derived in different ways, and the correct conclusions regarding instability were obtained.

Unlike the supported pipes conveying fluid, which are conservative in the absence of dissipation, however, a cantilevered pipe conveying fluid is a nonconservative system, which, for sufficiently high flow velocity, would lose stability by flutter of the single-degree-of-freedom (SDOF) type[8]. After the first study of Bourrières[9] on the stability of cantilevered pipes conveying fluid, Benjamin[10, 11] examined the dynamics of articulated cantilevers conveying fluid, but with a discussion of the continuous system. Paidoussis[12] and Gregory & Paidoussis[13, 14] extended Benjamin's work to the cases of continuously flexible pipes conveying fluid. They determined the conditions of instability via quasi-analytical and numerical solutions of the partial differential equation. These solutions were also compared with experimental results.

After Gregory & Paidoussis's work[13, 14], there have been a great number of studies of modified forms of the basic system of a cantilevered pipe conveying fluid. The fluid-conveying cantilevers were modified by adding different types of spring supports at various locations, by adding one or more additional masses at different locations, and so on. It was found that, under certain situations, these modifications could effectively change the dynamical behaviors of the cantilevered system.

The dynamical stability of cantilevered pipes with additional point masses have been studied by Hill & Swanson [15], Chen & Jendrzejczyk [16], Jendrzdjczyk & Chen [17], Sugiyanma et al.[18], Silva[19], Paidoussis et al.[20-23] and several other researchers[24-27]. Hill & Swanson[15] found that, in most cases,

* Corresponding author. E-mail: wanglindds@mail.hust.edu.cn

the additional masses destabilize the pipe system; however, adding a mass at mid-point is always stabilizing. Rinaldi and Paidoussis[22] devised an end-piece with four side holes for cantilevered pipes conveying fluid. The end-piece may be viewed as a special mass attachment, due to which the effective centrifugal term in the equation of motion vanishes. Therefore, the cantilevered pipe is unconditionally stable even for sufficiently high flow velocity. Based on the work of Rinaldi and Paidoussis[22], Wang and Dai[24] further considered the dynamics of fluid-conveying pipes fitted with an additional end-piece consisting of two symmetric elbows, which can enhance the stability of pipes conveying fluid, for both supported and clamped-free boundary conditions. Recently, Yang et al.[25] initiated to numerically examine the nonlinear responses of pinned-pinned pipes with an attached nonlinear energy sink (NES). The effect of NES on the pinned-pinned pipe is modelled by a cubic spring linked with a mass. It was shown that the NES can robustly absorb and dissipate a major portion of the vibrational energy of the pipe. Based on the work of Yang et al.[25], Mamaghani et al.[28] studied the oscillation responses of clamped-clamped pipe conveying fluid subjected to an external harmonic force with an attached NES. They found that the best position for the NES attachment is the middle point of the pipe and excellent suppression effects on the pipe system could be obtained. Song et al.[29] installed a Pounding Tuned Mass Damper (PTMD) on an M-shape pipeline system. The vibration control performance of PTMD for pipeline structure was studied by both experimental and numerical analysis. Rechenberger and Mair[30] proposed a mathematical models of Tuned Mass Damper (TMD) by the utilization of Microsoft Excel spreadsheet calculations. Their studies provided a practical guidance on the TMD design for controlling resonant vibrations of pipeline structures. Very recently, Zhou et al.[31] numerically investigated the stability and nonlinear responses of a cantilevered pipe conveying fluid with an NES attachment. The effects of damping, mass ratio and location of the NES were explored. Amongst the valuable studies reviewed here, the various methods for suppress the vibration and enhance the stability of fluid-conveying pipes have their advantage and deficiency. For instance, the special end-piece with four holes proposed in[22] can greatly enhance the stability of fluid-conveying pipe system but this special end-piece must be placed at the free end of the pipe; the NES device for suppressing the vibration of fluid-conveying pipes can transfer energy to the additional mass but sometimes it also may greatly increase the oscillations amplitudes of the pipe[30]; the study by Hill & Swanson[15] showed that an additional mass always has a destabilizing effect on the stability of a fluid-conveying pipe system.

From the work mentioned in the foregoing, it is natural to ask the question whether the dynamical stability of a cantilever conveying fluid can be improved by adding an attachment consisting of both linear spring and mass in its construction. To the authors' knowledge, the literature on this topic is limited.

In the current work, we focus our attention on the effect of a linear dynamic vibration absorber (DVA) on the dynamical stability of cantilevered pipes conveying fluid. It should be stressed that the NES proposed by Zhou et al.[31] consists of a nonlinear spring and a mass. In contrast, the additional attachment considered in this paper consists of a 'linear' spring and a mass. We will quasi-analytically investigate the effects on stability and post-instability responses of the location, damping coefficient, spring stiffness and mass ratio of the additional DVA. Some truly fascinating dynamical behaviors have been found in such a dynamical system, as will be shown below.

2. Governing equations

A schematic diagram of a cantilevered pipe conveying fluid with an additional DVA is shown in Fig. 1. The spring-mass attachment is devised at $x = x_b \leq L$, where L is the overall pipe length. It is assumed that the pipe is horizontal and the motions are in a horizontal plane.

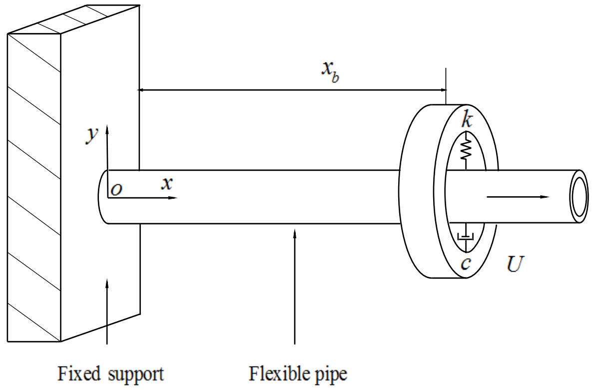

Fig. 1. Schematic of cantilever conveying fluid with an additional DVA

The pipe's lateral displacement is denoted by $W(s,t)$ along the y axes, with s being the curvilinear coordinate along the length of the pipe and t being the time. Following the derivation of Semler[32] and Zhang et al.[33], by considering the effect of DVA[31], the equation of motion of the pipe takes the form

$$
\begin{aligned}
&(m+M)\ddot{W} + 2MU\dot{W}'\left(1+W'^2\right) + MU^2\left(1+W'^2\right)W'' \\
&+EI\left[W''''\left(1+W'^2\right) + 4W'W''W''' + W''^3\right] + \psi EI\dot{W}'''' \\
&-W''\left[\begin{aligned}&\int_s^L\int_0^s (m+M)\left(\dot{W}' + W'\ddot{W}''\right)\mathrm{d}s\mathrm{d}s \\ &+\int_s^L\left(2MUW'\dot{W}' + MU^2W'W''\right)\mathrm{d}s\end{aligned}\right] \\
&+W'\int_0^s (m+M)\left(\dot{W}'^2 + W'\ddot{W}''\right)\mathrm{d}s \\
&-\left(K\left(V-W_b\right) + C\left(\dot{V}-\dot{W}_b\right)\right)\delta\left(s-s_b\right) = 0
\end{aligned}
\tag{1}
$$

where the overdot and prime denote the derivative with respect to t and s, respectively; EI is the flexural rigidity of the pipe, Ψ is the Kelvin-Voigt damping coefficient of the pipe; M is the mass of the internal fluid per unit length, U is the steady flow velocity, m is the mass of the empty pipe per unit length; W_b is the lateral deflection of the pipe at the location of the spring-mass attachment; K is the stiffness of the spring, C is the damping coefficient of the damper, V is the displacement of the additional mass; and $\delta(s - s_b)$ is the Dirac delta function with s_b denoting the location of DVA.

The governing equation of the DVA is given by

$$
m_1\ddot{V} + K\left(V-W_b\right) + C\left(\dot{V}-\dot{W}_b\right) = 0 \tag{2}
$$

in which m_1 is the mass of the attached rigid body.

Defining the following quantities

$$\xi = \frac{s}{L}, w = \frac{W}{L}, v = \frac{V}{L}, \tau = \left(\frac{EI}{m+M}\right)^{1/2}\frac{t}{L^2}, u = \left(\frac{M}{EI}\right)^{1/2} UL,$$

$$\beta = \frac{M}{M+m}, \varphi = \left(\frac{EI}{m+M}\right)^{1/2}\frac{\psi}{L^2}, \alpha = \frac{m_1}{(M+m)L}, k = \frac{KL^3}{EI},$$

$$c = \frac{CL}{\left[(m+M)EI\right]^{1/2}}$$

Eqs. (1) and (2) may be written in the dimensionless form

$$\begin{aligned} &w'''' + \varphi\dot{w}'''' + \ddot{w} + 2u\sqrt{\beta}\dot{w}' + u^2 w'' + N(w) \\ &-\left(k\left(v - w_b\right) + c\left(\dot{v} - \dot{w}_b\right)\right)\delta\left(\xi - \xi_b\right) = 0 \end{aligned} \tag{3}$$

in which the nonlinear term $N(w)$ is given by

$$\begin{aligned} N(w) &= 2u\sqrt{\beta}\dot{w}'w''^2 + w''u^2w'^2 + 3w'w''w''' + w''^3 \\ &+ w'\int_0^\xi \left\{\dot{w}'^2 - 2u\sqrt{\beta}w'\dot{w}'' - u^2 w'w''' + w''w''''\right\}\mathrm{d}\xi \\ &- w''\int_\xi^1\int_0^\xi \left[\dot{w}'^2 - 2u\sqrt{\beta}w'\dot{w}'' - u^2 w'w''' + w''w''''\right]\mathrm{d}\xi\mathrm{d}\xi \\ &- w''\int_\xi^1 \left(2u\sqrt{\beta}w'\dot{w}' + u^2 w'w'' + w''w'''\right)\mathrm{d}\xi \end{aligned} \tag{4}$$

$$\alpha\ddot{v} + k\left(v - w_b\right) + c\left(\dot{v} - \dot{w}_b\right) = 0 \tag{5}$$

where the prime and overdot on each variable now denotes the derivative with respect to ξ and τ, respectively.

3. Galerkin Method

The infinite-dimensional pipe model can be discretized by several effective methods, such as Galerkin approach[34-36] and differential quadrature method[37, 38]. In the following simulation, the partial differential equations are discretized by using a Galerkin approximation, with the the eigenfunctions of a plain cantilevered beam, $\phi_r(\xi)$, as the base functions, with $q_r(\tau)$ being the corresponding generalized coordinates; thus, the displacement of the pipe may be written as

$$w(\xi,\tau) = \sum_{r=1}^{N}\phi_r(\xi)q_r(\tau) \tag{6}$$

where N is the number of basis functions used in the discretization. Substituting expression (6) into Eqs. (3) and (5), multiplying by $\phi_i(\xi)$ and integrating from 0 to 1, one obtains the following ordinary differential equations

$$[\mathbf{M}]\begin{Bmatrix}\ddot{\mathbf{q}}\\ \ddot{\mathbf{v}}\end{Bmatrix} + [\mathbf{C}]\begin{Bmatrix}\dot{\mathbf{q}}\\ \dot{\mathbf{v}}\end{Bmatrix} + [\mathbf{K}]\begin{Bmatrix}\mathbf{q}\\ \mathbf{v}\end{Bmatrix} + \left\{\mathbf{f}_{nonl}\right\} = \{\mathbf{0}\} \tag{7}$$

where the overdot now denotes the total derivative with respect to time τ. In Eqs. (7), [**M**], [**C**] and [**K**] are the mass, damping and stiffness matrices for the linear parts and $\mathbf{f}_{nonl}$ is the nonlinear term associated with various nonlinearities of the pipe. In this study, a four-mode Galerkin approximation will be utilized (N=4) since the stability of the pipe system is usually associated with the lowest several modes.

By neglecting the nonlinear terms in Eqs. (7), the eigenvalues of pipe system may be obtained by analyzing a generalized eigenvalue problem. According to the obtained eigenvalues in each mode, the stability of the fluid-conveying pipe with DVA can be determined. When the pipe system becomes unstable, the post-instability responses of the pipe can be predicted by numerically solving the nonlinear equations of (7) via a fourth-order Runge-Kutta iteration algorithm.

4. Results

In this section, the main aim of the calculations is to explore the effect of DVA on the dynamical stability and the nonlinear responses of the pipe system. For that purpose, the evolution of eigenvalues for the pipe and the attached mass with increasing flow velocity will be displayed first. Based on the analysis regarding instability, the nonlinear responses of the pipe and the mass will be then analyzed. Results will be presented for the cantilevered pipe and the mass with various system parameters, mainly in the form of Argand diagrams, bifurcation diagrams and phase portraits.

4.1. Model validation

To check the correctness of the quasi-analytical solutions, the case φ= 0.001 and β=0.213 with no DVA is revisited first. The dynamical behaviors of this basic system with increasing dimensionless flow velocity, u, are illustrated by the Argand diagram of Fig. 2. It is recalled that Re(ω) is the dimensionless oscillation frequency, while Im(ω) is related to the damping of the whole system. It is seen that the system is stable for small flow velocity since fluid flow induces damping in all modes of the system. For higher u, Im(ω) in the second mode of the system begins to decrease and eventually evolves to negative values; thus, flutter instability would occur at $u_{cr} \approx 5.8$. It can be seen that the results shown in Fig. 2 are almost the same as those obtained by Gregory & Païdoussis[13] and Paidoussis & Issid[39], thus indicating that the quasi-analytical solutions in this work are correct.

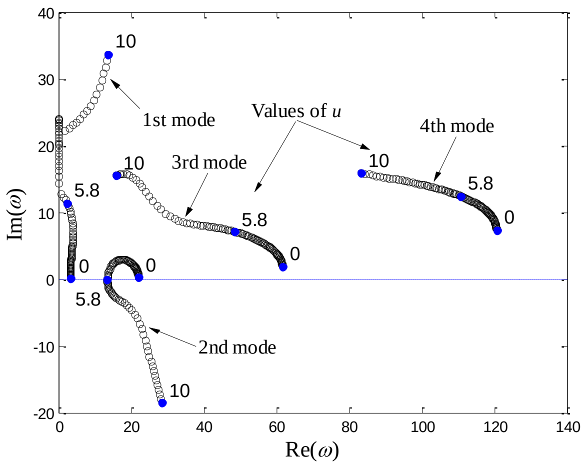

Fig. 2. Argand diagram for a cantilevered pipe conveying fluid without DVA. (u_{cr}=5.8) It is seen that the critical flow velocity is u_{cr}=5.8.

4.2. Effect of dynamic vibration absorber on the critical flow velocity

In this subsection, the critical flow velocity of the pipe with different parameters of DVA will be analyzed in some detail. Figs. 3-8 show the critical flow velocities of the system with varied physical and geometrical parameters of the DVA for φ= 0.001, α = 0.1, β=0.213.

The dimensionless critical flow velocities u_{cr} of the system as a function of dimensionless stiffness and location of DVA are plotted in Fig. 3, where the red region is obviously observed in the ranges of 10< k <20 and 0.4 < ξ_b <0.6. That is to say, in these ranges of k and ξ_b, the dimensionless critical flow velocity of the system become higher and its peak value can be achieved. Figs. 3(a)-(c) correspond to three different dimensionless damping coefficients: c=0.1, 0.3 and 0.5, respectively. It is seen that the red region of Fig. 3(c) is darker than that of Figs. 3(a) and (b). This means that, when k ranges from 0 to 60 and ξ_b ranges from 0 to 1, the higher critical flow velocities of the pipe system in the presence of DVA could be obtained in the case of larger damping of DVA.

Fig. 4 shows that the dimensionless critical flow velocities of the system as a function of dimensionless stiffness and location of DVA for three different values of mass ratio (α). It is obvious that the peak value of critical flow velocity of the system appear at ξ_b≈0.5. As shown in Figs 4(a)-(c), with the increment of dimensionless mass ratio, a larger stiffness of DVA is required to achieve higher crtitical flow velocity.

The dimensionless critical flow velocities of the system as a function of dimensionless stiffness and mass ratio of DVA are shown in Fig. 5, for a given value of DVA location. Inspecting Figs. 5(a)-(c), a feature is easy to found: with the increment of damping of DVA, the stiffness and the mass ratio of DVA needs to be increased to achieve higher critical flow velocity.

Figs. 6(a)-(c) plot the results of critical flow velocities for a given damping coefficient and three different values of DVA location. It is found that, when the attached location of DVA is closer to the free end, the stiffness of DVA needs to be decreased in order to obtain higher critical flow velocity. Upon comparing the three diagrams of Fig. 6, again, it is shown that higher critical flow velocity can be realized at about ξ_b =0.5.

Figs. 7(a)-(c) show the critical flow velocities of the system for a given DVA location and three different values of mass ratio. It is observed that, with the increment of mass ratio α, the stiffness and damping coefficient need to be increased to obtain higher critical flow velocity. Among the three cases shown in Fig. 7, the maximum critical flow velocity appears at α=0.1.

In Fig. 8, the dimensionless critical flow velocities as a function of dimensionless stiffness and damping coefficient of DVA for α = 0.1 and three values of ξ_b are shown. Once again, it is seen that when the location of the DVA is close to the midpoint of the pipe, the stability of the pipe can be better enhanced by using the DVA.

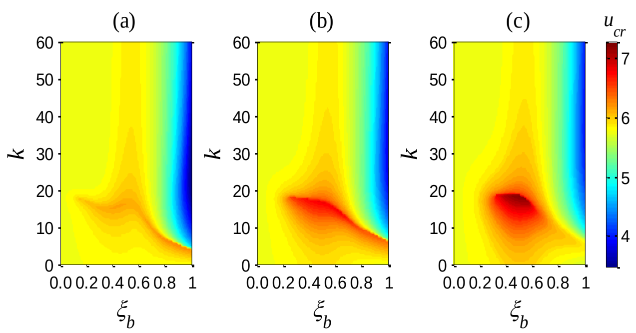

Fig. 3. Dimensionless critical flow velocities u_{cr} of the system as a function of dimensionless stiffness and location of DVA for φ= 0.001, α = 0.1, β=0.213: (a) c= 0.1, (b) c= 0.3 and (c) c= 0.5.

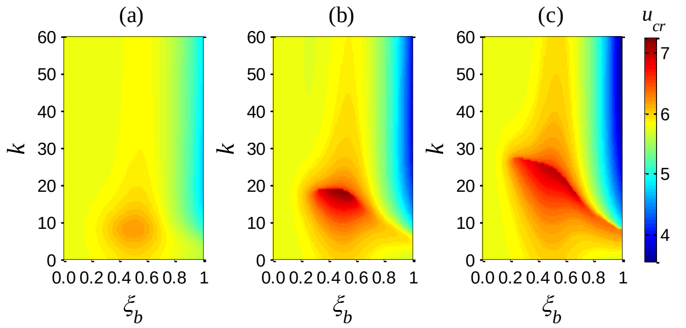

Fig. 4. Dimensionless critical flow velocities u_{cr} of the system as a function of dimensionless stiffness and location of DVA for φ= 0.001, c= 0.5, β=0.213: (a) α = 0.05, (b) α = 0.1 and (c) α = 0.15

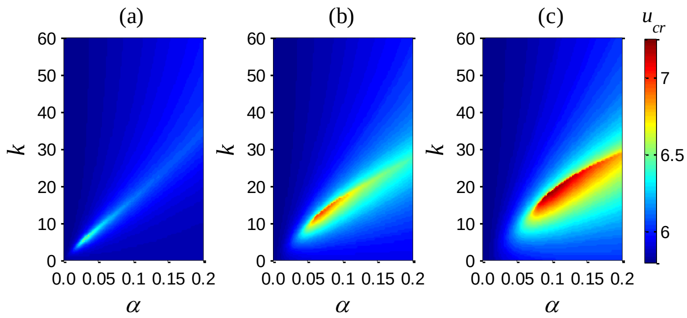

Fig. 5. Dimensionless critical flow velocities ucr of the system as a function of dimensionless stiffness and mass ratio of DVA for φ= 0.001, ξb=0.5, β=0.213: (a) c= 0.1, (b) c= 0.3 and (c) c= 0.5.

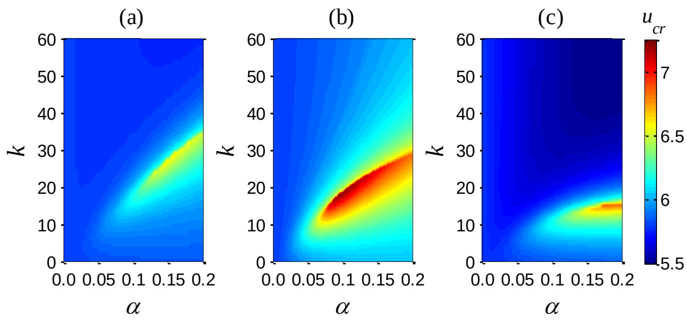

Fig. 6. Dimensionless critical flow velocities u_{cr} of the system as a function of dimensionless stiffness and mass ratio of DVA for φ= 0.001, c= 0.5, β=0.213: (a) ξ_b = 0.25, (b) ξ_b = 0.5 and (c) ξ_b = 0.75.

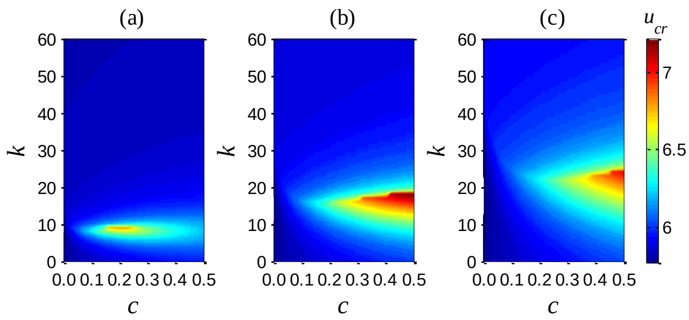

Fig. 7. Dimensionless critical flow velocities u_{cr} of the system as a function of dimensionless stiffness and damping of DVA for φ= 0.001, ξ_b=0.5, β=0.213: (a) α = 0.05, (b) α = 0.1 and (c) α = 0.15.

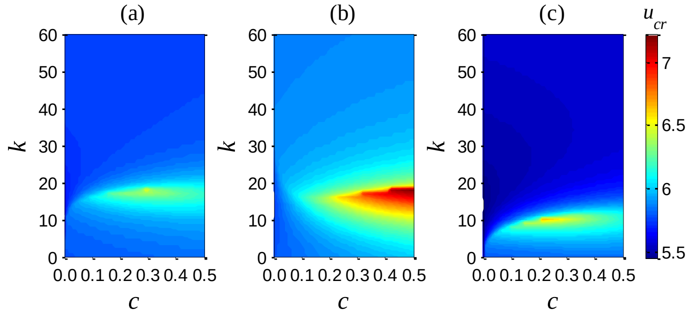

Fig. 8. Dimensionless critical flow velocities u_{cr} of the system as a function of dimensionless stiffness and damping of DVA for φ= 0.001, α = 0.1, β=0.213: (a) ξ_b = 0.25, (b) ξ_b = 0.5 and (c) ξ_b = 0.75.

To explore the basic stability mechanism of the pipe in the presence of DVA, some typical results of Argand diagrams for the dynamical system are further constructed. The Argand diagrams of a cantilevered pipe conveying fluid in the presence of DVA for several different values of k and a set of other system parameters (φ= 0.001, α = 0.1, c= 0.5, β=0.213 and ξ_b = 0.5) are plotted in Figs. 9-16. In these figures, the evolution of the lowest four non-dimensional eigen-frequencies of the pipe, and the evolution of the non-dimensional eigen-frequencies of the DVA mass are shown.

The Argand diagram for k = 14 is shown in Fig. 9. It is immediately seen that the flutter instability of the pipe occurs at about u_{cr}=6.9 in the second mode. For u ranges from 0 to 10, all values of Im(ω) of the DVA are above the zero axis, indicating that instability of the DVA is impossible in this case. Thus, the critical flow velocity of the pipe attached with DVA is equal to 6.9, which is much higher than the critical value of the same pipe but without DVA. Fig. 10 shows the Argand diagram for k = 18. It can be seen that the evolution of the lowest five non-dimensional eigen-frequencies of the system shown in Fig. 10 is fairly similar as that of Fig. 9. The flutter instability of the system occurs at about u_{cr} =7.2. The Argand diagram for k = 19 is shown in Fig. 11. In this case, interestingly, with the increment of u, the values of Im(ω) of the DVA convert from positive to negative, and immediately convert to positive again. That is to say, the DVA would lose stability at the critical flow velocity of u=6.6 while the flutter instability of the pipe occurs at u=7.3. In such case, therefore, the critical flow velocity of the system would be u_{cr} =6.6. Fig. 12 shows the Argand diagram of the cantilevered pipe conveying fluid with DVA for k = 42. It is found that the DVA loses stability at u_{cr} =5.9 and the pipe lose stability at about u=8.2.

The Argand diagram for k = 43 is shown in Fig. 13 and the critical flow velocity for flutter instability is almost the same as that shown in Fig. 12. However, the eigenvalue locus for DVA and the second-mode eigenvalue locus for the pipe can be extremely close. The Argand diagram for k = 44 is shown in Fig. 14. Compared with the evolution of non-dimensional eigen-frequencies of the system plotted in Fig. 12 or 13, the eigenvalue locus for DVA and the second-mode eigenvalue locus for the pipe is interchanged when the flow velocity becomes high. The results shown in Fig. 14 indicate that the DVA loses stability at u_{cr} =5.9 and the pipe lose stability at u=8.2. When the stiffness of the DVA is further increased to k=55, the critical flow velocity of the system shown in Fig. 15 is found to be u_{cr} =5.9. In that case, the DVA will keep stability because all values of Im(ω) of the DVA are positive. Indeed, when the dimensionless stiffness of the DVA is further increased but below 60, the critical flow velocity of the system does not change (u_{cr} =5.9), as can be seen from the results shown in Fig. 16 for k=60.

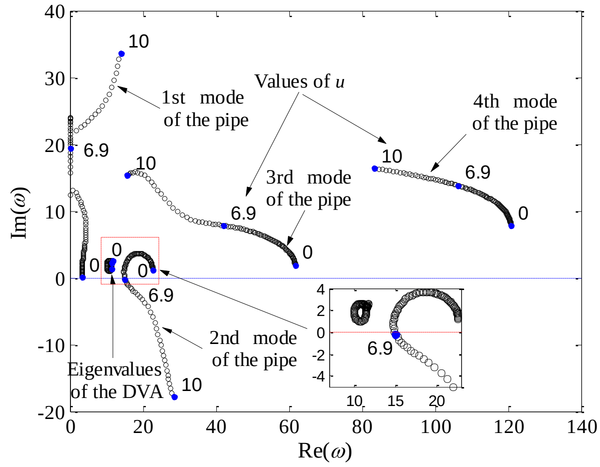

Fig. 9. Argand diagram for a cantilevered pipe conveying fluid with DVA for k = 14, φ= 0.001, α = 0.1, c= 0.5, β=0.213, ξ_b = 0.5. It is seen that the critical flow velocity for the whole system is u_{cr}=6.9.

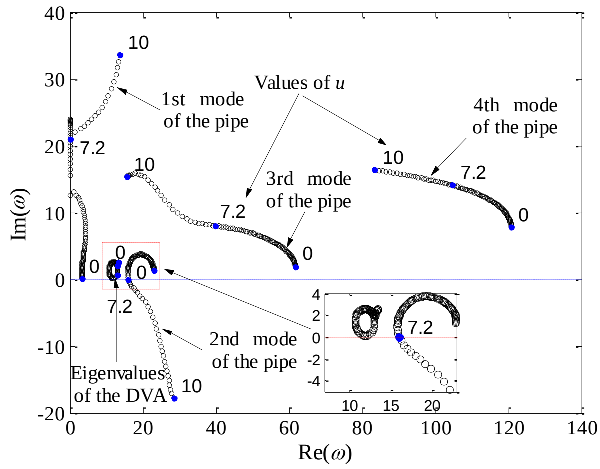

Fig. 10. Argand diagram for a cantilevered pipe conveying fluid with DVA for k = 18, φ= 0.001, α = 0.1, c= 0.5, β=0.213, ξ_b = 0.5. It is seen that the critical flow velocity for the whole system is u_{cr}=7.2.

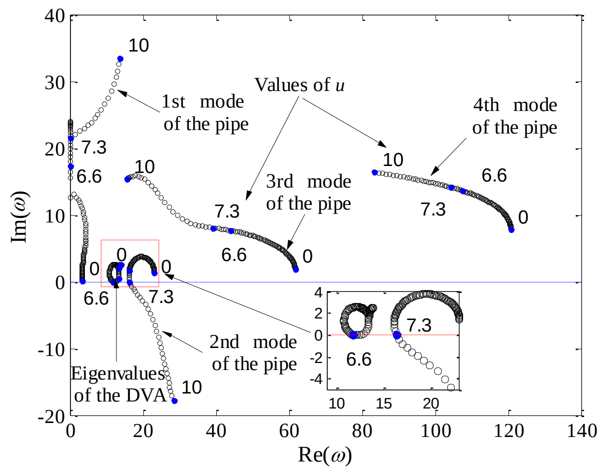

Fig. 11. Argand diagram for a cantilevered pipe conveying fluid with DVA for k = 19, φ= 0.001, α = 0.1, c= 0.5, β=0.213, ξ_b = 0.5. It is seen that the critical flow velocity for the whole system is u_{cr}= 6.6.

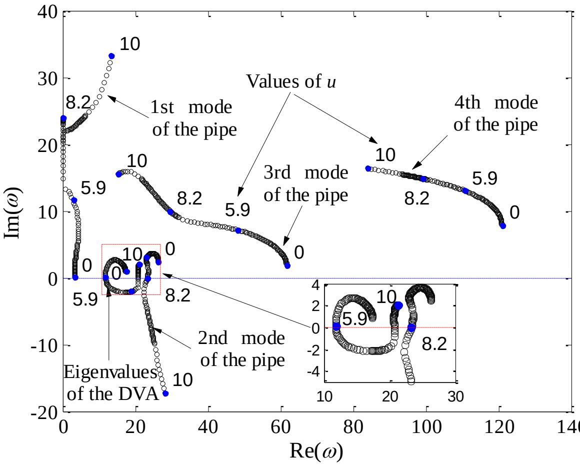

Fig. 12. Argand diagram for a cantilevered pipe conveying fluid with DVA for k = 42, φ= 0.001, α = 0.1, c= 0.5, β=0.213, ξ_b = 0.5. It is seen that the critical flow velocity for the whole system is u_{cr}= 5.9.

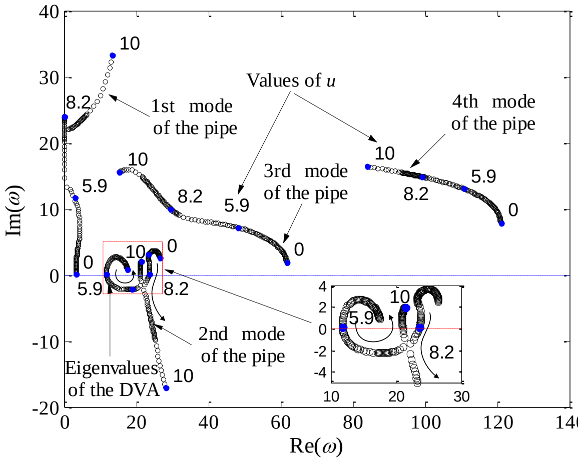

Fig. 13. Argand diagram for a cantilevered pipe conveying fluid with DVA for k = 43, φ= 0.001, α = 0.1, c= 0.5, β=0.213, ξ_b = 0.5. It is seen that the critical flow velocity for the whole system is u_{cr}= 5.9.

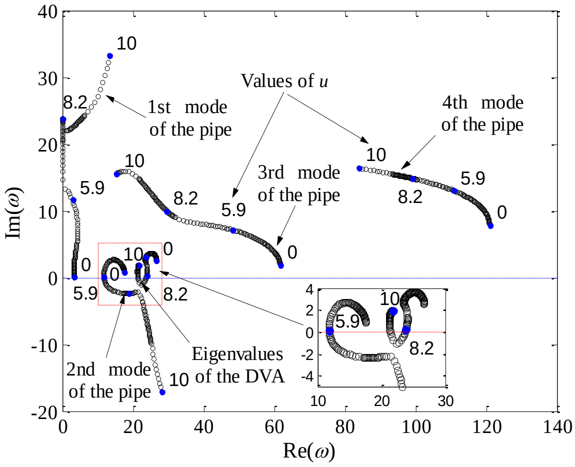

Fig. 14. Argand diagram for a cantilevered pipe conveying fluid with DVA for k = 44, φ= 0.001, α = 0.1, c= 0.5, β=0.213, ξ_b = 0.5. It is seen that the critical flow velocity for the whole system is u_{cr}= 5.9.

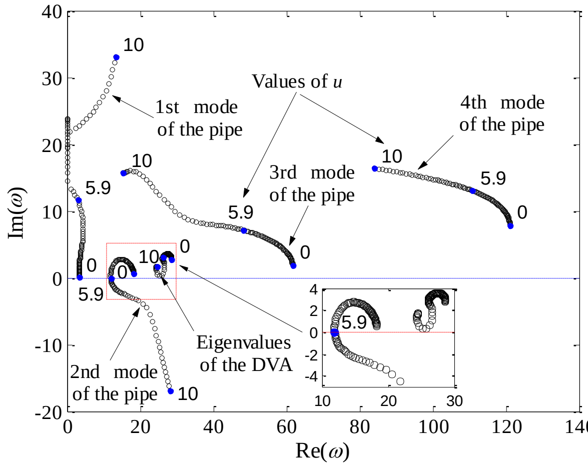

Fig. 15. Argand diagram for a cantilevered pipe conveying fluid with DVA for k = 55, φ= 0.001, α = 0.1, c= 0.5, β=0.213, ξ_b = 0.5. It is seen that the critical flow velocity for the whole system is u_{cr}= 5.9.

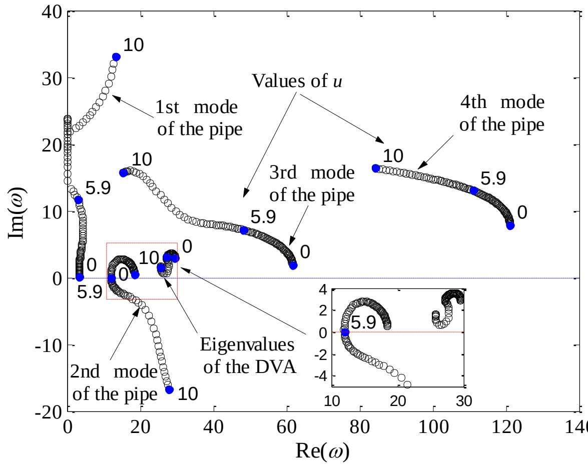

Fig. 16. Argand diagram for a cantilevered pipe conveying fluid with DVA for k = 60, φ= 0.001, α = 0.1, c= 0.5, β=0.213, ξ_b = 0.5. It is seen that the critical flow velocity for the whole system is u_{cr}= 5.9.

4.3. Effect of DVA on nonlinear oscillations of the pipe

In this subsection, our attention will be focused on the nonlinear oscillations of the cantilevered pipe conveying fluid with DVA when the flow velocity is successively increased. It will be shown that this modified system could display some fascinating dynamical behaviors. The numerical results are presented in the form of phase portraits and bifurcation diagrams.

As discussed in the foregoing (see Fig. 3), when the system parameters are set as φ= 0.001, ξ_b =0.5, c=0.5, α = 0.1, k=18 and β=0.213, the whole system can obtain the maximum critical flow velocity. In this case, the bifurcation diagrams for the system are plotted in Fig. 17. It is obvious that the flutter instability of the pipe with DVA occurs at a higher flow velocity if compared with that of the pipe without DVA. More importantly, for all flow velocities, the oscillation amplitudes of the pipe with DVA are generally smaller than that of the pipe without DVA. When the flow velocity becomes high (e.g., u= 10), the oscillation amplitudes of the pipe with and without DVA has no obvious difference.

From the results for k=19 shown in Fig. 11, it is noted that the DVA becomes unstable at a critical flow velocity lower than the flow velocity for flutter instability of the pipe. Thus, one might have thought that the system for k=19 could generate some different dynamical behavior if compared with the case of k=18.

This is true, as shown in Fig. 18, where the system loses instability at u_{cr} =6.6, then regains stability at about u=7, and finally become unstable with further increasing flow velocity. As shown in Fig. 18(a), the oscillation amplitudes of the pipe change from zero to nonzero at about u=7.3. The same phenomenon can be observed in Fig. 18(b) for the dynamic response of the DVA.

In the case of k=30, the bifurcation diagrams for the system with internal flow velocity as the variable parameter are plotted in Fig. 19. In this case, the suppression of oscillation amplitudes of the pipe with DVA can only be realized in a certain range of flow velocity: 7.6 < u < 10. The bifurcation diagrams for another larger stiffness value of k=42 are shown in Fig. 20. In the range of 6.5 < u <8.2 approximately, the oscillation amplitudes of the pipe with DVA are slightly larger than that of the pipe without DVA, indicating that the DVA may have a negative effect on the pipe's responses. In the range of 8.2 < u <10.5 approximately, the oscillation amplitudes of the pipe with DVA are slightly smaller than that of the pipe without DVA. That is to say, for φ= 0.001, ξ_b =0.5, c=0.5, α = 0.1 and β=0.213, the most effective influence of DVA on the oscillation responses of the cantilevered pipe conveying fluid would occur at k=18, as can be observed in Figs. 17-20.

In order to further understand the dynamic responses of the cantilevered pipe with and without DVA, some phase portraits for several typical flow velocities are plotted in Figs. 21-23, for k=19. The phase portraits shown in Fig. 21 are for u=6.2. It is noted that the pipe without DVA undergoes a symmetric limit cycle (Fig. 21(a)) while the motion of the pipe with DVA is toward to a fixed point (Fig. 21(b)). In the case of u=6.6, it is clearly seen from Fig. 22 that the pipe undergoes a limit cycle motion, either without or with the DVA. Moreover, the displacement and velocity amplitudes of the pipe without DVA are much larger than the counterpart of the same pipe with DVA. Fig. 23 shows the phase portraits of the pipe without and with DVA for u=7.1. It is obvious that the pipe without DVA undergoes a limit cycle motion while the trajectory of the pipe with DVA is towards to a fixed point.

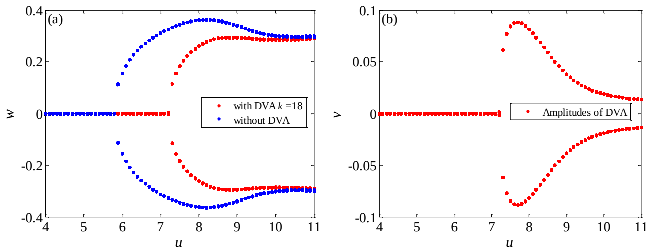

Fig. 17. Bifurcation diagram of the pipe system displacements with internal flow velocity u being the variable parameter for: φ= 0.001, ξ_b =0.5, c=0.5, k=18, α = 0.1, β=0.213: (a) tip-end displacements of the pipe and (b) displacements of the dynamic vibration absorber.

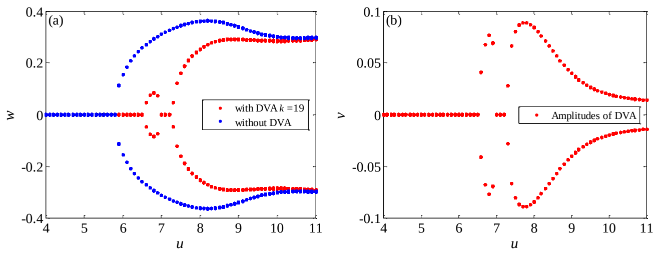

Fig. 18. Bifurcation diagram of the pipe system displacements with internal flow velocity u being the variable parameter for: φ= 0.001, ξ_b =0.5, c=0.5, k=19, α = 0.1, β=0.213: (a) tip-end displacements of the pipe and (b) displacements of the dynamic vibration absorber.

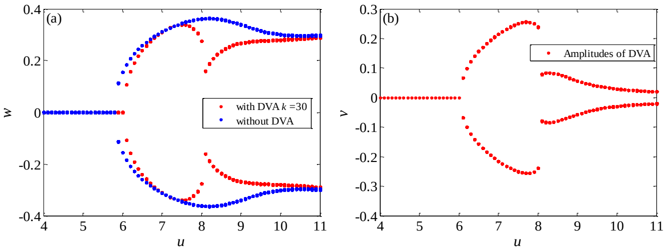

Fig. 19. Bifurcation diagram of the pipe system displacements with internal flow velocity u being the variable parameter for: φ= 0.001, ξ_b =0.5, c=0.5, k=30, α = 0.1, β=0.213: (a) tip-end displacements of the pipe and (b) displacements of the dynamic vibration absorber.

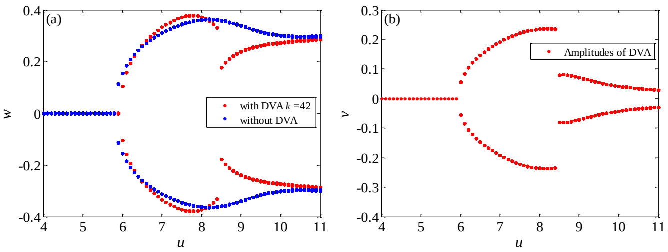

Fig. 20. Bifurcation diagram of the pipe system displacements with internal flow velocity u being the variable parameter for: φ= 0.001, ξ_b =0.5, c=0.5, k=42, α = 0.1, β=0.213: (a) tip-end displacements of the pipe and (b) displacements of the dynamic vibration absorber.

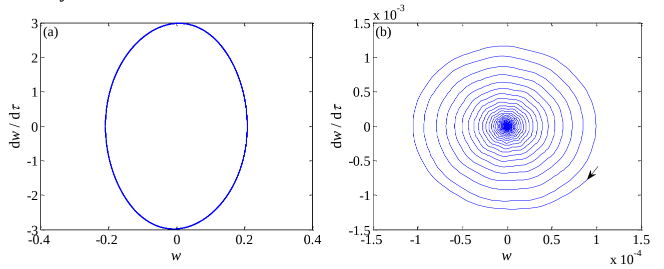

Fig. 21. Phase portraits for the tip-end response of the cantilevered pipe for: φ= 0.001, ξ_b =0.5, c=0.5, k=19, α = 0.1, β=0.213 and u=6.2: (a) without DVA and (b) with DVA.

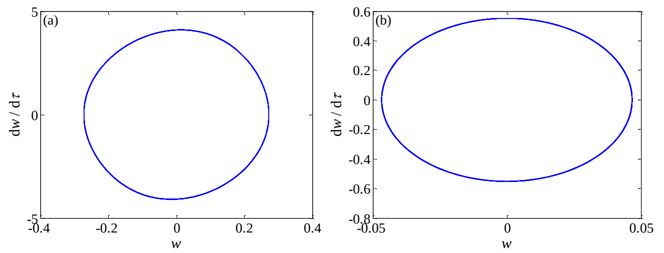

Fig. 22. Phase portraits for the tip-end response of the cantilevered pipe for: φ= 0.001, ξ_b =0.5, c=0.5, k=19, α = 0.1, β=0.213 and u=6.6: (a) without DVA and (b) with DVA.

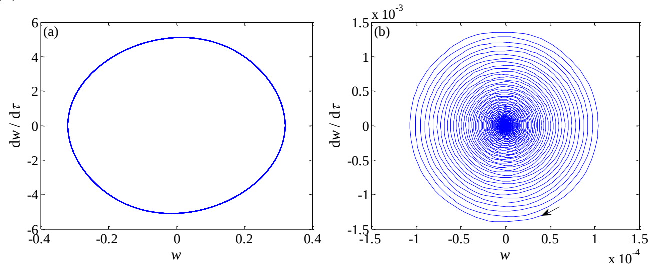

Fig. 23. Phase portraits for the tip-end response of the cantilevered pipe for: φ= 0.001, ξ_b =0.5, c=0.5, k=19, α = 0.1, β=0.213 and u=7.1: (a) without DVA and (b) with DVA.

4.4. Discussion

With regard to the foregoing analysis, one important point should be stressed. We have found that the presence of DVA has a significant effect on the dynamical stability of the pipe. The critical flow velocity of the pipe may become higher, which implies that the stability of the pipe can be enhanced by using the DVA. More interestingly, in some cases, the critical flow velocity of the DVA is much lower than that of the pipe. This means that even if the pipe is stable with no oscillations, the DVA may become unstable and oscillation is possible. In such a case, the energy gained from the fluid flow could be further transferred from the pipe to the DVA, causing the DVA to oscillate. In summary, the DVA devised in the work has the ability to absorb energy from the pipe and hence can enhance the stability of the pipe conveying fluid.

5. Conclusions

The present study is concerned with the dynamical stability and nonlinear responses of a cantilevered pipe conveying fluid with a DVA added somewhere along the pipe length. We found that the pipe loses stability by flutter when the flow velocity exceeds a certain critical value. The damping coefficient, stiffness, location, and weight of the additional DVA do influence this instability. Under certain conditions, the critical flow velocity of the pipe can be remarkably increased by having a DVA, thus enhancing the stability of the pipe system.

Since the mass would gain energy from the pipe, in many cases, the critical flow velocity of the pipe with DVA is higher than that of the pipe without DVA. Therefore, the results obtained in this paper provide a possible way to design energy absorbers (or energy transfer devices) for fluid-conveying pipes by adding DVAs somewhere along the pipe length.

Acknowledgments

The authors gratefully acknowledge the support provided by the National Natural Science Foundation of China (No. 11622216).

References

[1] M. P. Paidoussis, G. X. Li, Pipes conveying fluid: a model dynamical problem, *Journal of Fluids and Structures,* Vol. 7, No. 2, pp. 137-204, 1993.

[2] M. P. Paidoussis, The canonical problem of the fluid-conveying pipe and radiation of the knowledge gained to other dynamics problems across Applied Mechanics, *Journal of Sound and Vibration,* Vol. 310, No. 3, pp. 462-492, Feb 10, 2008.

[3] Y. Yang, J. Wang, Y. Yu, Wave propagation in fluid-filled single-walled carbon nanotube based on the nonlocal strain gradient theory, *Acta Mechanica Solida Sinica,* Vol. 31, No. 4, pp. 484-492, 2018.

[4] M. Hosseini, H. H. Gorgani, M. Shishesaz, A. Hadi, Size-dependent stress analysis of single-wall carbon nanotube based on strain gradient theory, *International Journal of Applied Mechanics,* Vol. 9, No. 06, pp. 1750087, 2017.

[5] V. Feodos'Ev, Vibrations and stability of a pipe when liquid flows through it, *Inzhenernyi Sbornik,* Vol. 10, pp. 169-170, 1951.

[6] G. Housener, Bending vibration of a pipeline containing flowing fluid, *Journal of Applied Mechancis,* Vol. 19, pp. 205, 1952.

[7] F. I. Niordson, 1953, *Vibrations of a cylindrical tube containing flowing fluid*, Kungliga Tekniska Hogskolans Handlinar (Stockholm),

[8] R. D. Blevins, 1977, *Flow-induced vibration*, Van Nostrand Reinhold Co., New York

[9] F.-J. Bourrières, 1939, *Sur un phénomène d'oscillation auto-entretenue en mécanique des fluides réels*, E. Blondel La Rougery,

[10] T. B. Benjamin, Dynamics of a system of articulated pipes conveying fluid. I. Theory, *Proceedings of the Royal Society of London A: Mathematical, Physical and Engineering Sciences,* Vol. 261, No. 1307, pp. 457-486, 1961.

[11] T. B. Benjamin, Dynamics of a system of articulated pipes conveying fluid. II. Experiments, *Proceedings of the Royal Society of London A: Mathematical, Physical and Engineering Sciences,* Vol. 261, No. 1307, pp. 487-499, 1961.

[12] M. P. Paidoussis, *Oscillations of liquid-filled flexible tubes*, Thesis, University of Cambridge, 1963.

[13] R. W. Gregory, M. P. Paidoussis, Unstable oscillation of tubular cantilevers conveying fluid I. Theory, *Proc. R. Soc. Lond. A,* Vol. 293, No. 1435, pp. 512-527, 1966.

[14] R. W. Gregory, M. P. Paidoussis, Unstable oscillation of tubular cantilevers conveying fluid II. Experiments, *Proc. R. Soc. Lond. A,* Vol. 293, No. 1435, pp. 528-542, 1966.

[15] J. Hill, C. Swanson, Effects of lumped masses on the stability of fluid conveying tubes, *Journal of Applied Mechanics,* Vol. 37, No. 2, pp. 494-497, 1970.

[16] S. Chen, J. Jendrzejczyk, General characteristics, transition, and control of instability of tubes conveying fluid, *The Journal of the Acoustical Society of America,* Vol. 77, No. 3, pp. 887-895, 1985.

[17] J. A. Jendrzejczyk, S. S. Chen, Experiments on tubes conveying fluid, *Thin-Walled Structures,* Vol. 3, No. 2, pp. 109-134, 1985.

[18] Y. Sugiyama, H. Kawagoe, T. Kishi, S. Nishiyama, Studies on the Stability of Pipes Conveying Fluid: The Combined Effect of a Spring Support and a Lumped Mass, *JSME international journal. Ser. 1, Solid mechanics, strength of materials,* Vol. 31, No. 1, pp. 20-26, 1988.

[19] M. A. G. Silva, Influence of eccentric valves on the vibration of fluid conveying pipes, *Nuclear Engineering and Design,* Vol. 64, No. 1, pp. 129-134, 1981.

[20] M. P. Paidoussis, C. Semler, Non-linear dynamics of a fluid-conveying cantilevered pipe with a small mass attached at the free end, *International Journal of Non-Linear Mechanics,* Vol. 33, No. 1, pp. 15-32, 1998.

[21] Y. Modarres-Sadeghi, C. Semler, M. Wadham-Gagnon, M. P. Païdoussis, Dynamics of cantilevered pipes conveying fluid. Part 3: Three-dimensional dynamics in the presence of an end-mass, *Journal of Fluids and Structures,* Vol. 23, No. 4, pp. 589-603, 2007.

[22] S. Rinaldi, M. P. Paidoussis, Dynamics of a cantilevered pipe discharging fluid, fitted with a stabilizing end-piece, *Journal of Fluids and Structures,* Vol. 26, No. 3, pp. 517-525, 2010.

[23] M. H. Ghayesh, M. P. Paidoussis, Y. Modarres-Sadeghi, Three-dimensional dynamics of a fluid-conveying cantilevered pipe fitted with an additional spring-support and an end-mass, *Journal of Sound and Vibration,* Vol. 330, No. 12, pp. 2869-2899, 2011.

[24] L. Wang, H. L. Dai, Vibration and enhanced stability properties of fluid-conveying pipes with two symmetric elbows fitted at downstream end, *Archive of Applied Mechanics,* Vol. 82, No. 2, pp. 155-161, 2012/02/01, 2012.

[25] T. Z. Yang, X. D. Yang, Y. H. Li, B. Fang, Passive and adaptive vibration suppression of pipes conveying fluid with variable velocity, *Journal of Vibration and Control,* Vol. 20, No. 9, pp. 1293-1300, 2014.

[26] R. D. Firouz-Abadi, A. R. Askarian, M. Kheiri, Bending–torsional flutter of a cantilevered pipe conveying fluid with an inclined terminal nozzle, *Journal of Sound and*

Vibration, Vol. 332, No. 12, pp. 3002-3014, 2013/06/10/, 2013.

[27] G. S. Copeland, F. C. Moon, Chaotic flow-induced vibration of a flexible tube with end mass, *Journal of Fluids and Structures,* Vol. 6, No. 6, pp. 705-718, 1992/11/01/, 1992.

[28] A. E. Mamaghani, S. Khadem, S. Bab, Vibration control of a pipe conveying fluid under external periodic excitation using a nonlinear energy sink, *Nonlinear Dynamics,* Vol. 86, No. 3, pp. 1761-1795, 2016.

[29] G. B. Song, P. Zhang, L. Li, M. Singla, D. Patil, H. N. Li, Y. L. Mo, Vibration control of a pipeline structure using pounding tuned mass damper, *Journal of Engineering Mechanics,* Vol. 142, No. 6, pp. 04016031, 2016.

[30] S. Rechenberger, D. Mair, Vibration Control of Piping Systems and Structures Using Tuned Mass Dampers, *ASME 2017 Pressure Vessels and Piping Conference, Hawaii, USA*, Vol. PVP2017-65448, pp. V03BT03A035, 2017.

[31] K. Zhou, F. R. Xiong, N. B. Jiang, H. L. Dai, H. Yan, L. Wang, Q. Ni, Nonlinear vibration control of a cantilevered fluid-conveying pipe using the idea of nonlinear energy sink, *Nonlinear Dynamics*, pp. 1-22, 2018.

[32] C. Semler, Nonlinear dynamics and chaos of a pipe conveying fluid, *McGill University*, 1992.

[33] Y. W. Zhang, B. Yuan, B. Fang, L. Q. Chen, Reducing thermal shock-induced vibration of an axially moving beam via a nonlinear energy sink, *Nonlinear Dynamics,* Vol. 87, No. 2, pp. 1159-1167, 2017.

[34] L. Wang, Z. Y. Liu, A. Abdelkefi, Y. K. Wang, H. L. Dai, Nonlinear dynamics of cantilevered pipes conveying fluid: Towards a further understanding of the effect of loose constraints, *International Journal of Non-Linear Mechanics,* Vol. 95, pp. 19-29, 2017.

[35] Z. Y. Liu, L. Wang, X. P. Sun, Nonlinear Forced Vibration of Cantilevered Pipes Conveying Fluid, *Acta Mechanica Solida Sinica,* Vol. 31, No. 1, pp. 32-50, February 01, 2018.

[36] Z. Y. Liu, L. Wang, H. L. Dai, P. Wu, T. L. Jiang, Nonplanar vortex-induced vibrations of cantilevered pipes conveying fluid subjected to loose constraints, *Ocean Engineering,* Vol. 178, pp. 1-19, 2019.

[37] M. Mohammadi, M. Ghayour, A. Farajpour, Analysis of free vibration sector plate based on elastic medium by using new version of differential quadrature method, Vol. 3, No. 2, pp. 47-56, 2011.

[38] M. Danesh, A. Farajpour, M. Mohammadi, Axial vibration analysis of a tapered nanorod based on nonlocal elasticity theory and differential quadrature method, *Mechanics Research Communications,* Vol. 39, No. 1, pp. 23-27, 2012.

[39] M. P. Paidoussis, N. T. Issid, Dynamic stability of pipes conveying fluid, *Journal of sound and vibration,* Vol. 33, No. 3, pp. 267-294, 1974.